Sequential Ortho Effects: Characterization of Novel $[M - 35]^+$ Fragment Ions in the Mass Spectra of 2-Alkyl-4,6-dinitrophenols

John S. Riley and Tomas Baer
Department of Chemistry

G. Dean Marbury
Department of Environmental Science and Engineering,
University of North Carolina,
Chapel Hill, North Carolina, USA

High-resolution mass spectrometry (HRMS), hybrid tandem mass spectrometry (MS/MS) (EBqQ), and photoelectron–photoion coincidence (PEPICO) experiments were conducted to examine a possible ortho–ortho effect resulting in a novel $[M - 35]^+$ fragment ion in 2-alkyl-4,6-dinitrophenols. For compounds having ethyl or larger alkyl substituents, $[M - 35]^+$ was observed only when $[M - 18]^+$ ions were present, with the ortho nitro group being involved in the reaction to $[M - 35]^+$. For $[M - 18]^+$ and $[M - 35]^+$, HRMS results were consistent with losses of H_2O and H_2O + OH, respectively, whereas MS/MS results indicated a sequential reaction due to metastable dissociations. The appearance energy determined by PEPICO for $[M - 35]^+$ was found to be greater than the appearance energy for $[M - 18]^+$, thus supporting a sequential reaction. *(J Am Soc Mass Spectrom 1991, 2, 69–75)*

The ortho effect in ionic rearrangements refers to reactions that are unique to ortho substituents on aromatic rings. Such functional groups as phenol, acid, anhydride, ester, aldehyde, and ketone have been shown to exhibit ortho-effect reactions [1]. Specific examples include methoxy hydrogen atom transfer to an acetylenic carbon in 2-methoxyphenyl acetylene and 2-methoxydiphenyl acetylenes [2] and methyl hydrogen atom transfer in barbituric acids [3]. The term "ortho effect" is used because similar reaction products are, in general, absent in the isomeric meta and para compounds [1–6].

In particular, aromatic compounds containing a nitro group show pronounced ortho effects [4–12]. Some of the reported nitroaromatic ortho effects include hydrogen transfer to a nitro oxygen [6, 8], simple oxygen migration [4, 6, 8–10], nitro oxygen insertion into the ortho substituent [8], ring closure between the nitro group and the ortho substituent [4, 12], and other major skeletal rearrangements [11]. Ortho-effect reactions observed in the mass spectra of nitroaromatic compounds have often been explained by complex mechanisms in order to account for unusual fragment-ion structures [10].

On the basis of this nitroaromatic behavior, it seems that ionic fragmentations of 2-alkyl-4,6-dinitrophenols (2-alkyl-DNPs),

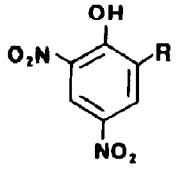

would exhibit ortho effects. Two of these compounds, dinoseb (2-*sec*-butyl-DNP) and dinex (2-cyclohexyl-DNP), are environmentally significant pesticides. This mass spectrometric investigation of the mechanism and energetics of the 2-alkyl-4,6-DNP ion dissociations was undertaken to determine the utility of ortho-effect products as a means of identifying these types of molecules.

The compounds studied were probed by high-resolution mass spectrometry (HRMS) and hybrid tandem mass spectrometry (MS/MS). In addition, one compound was studied by threshold photoelectron–photoion coincidence (PEPICO) time-of-flight (TOF) mass spectrometry, and the data were compared to the results of theoretical rate calculations. Finally, a mechanism for unusual fragment-ion production is proposed.

Address reprint requests to Tomas Baer, Department of Chemistry, University of North Carolina, Chapel Hill, NC 27599-3290.

1044-0305/91/$3.50

Received May 14, 1990
Accepted July 31, 1990

Experimental

The compounds 2-*sec*-butyl-DNP and 2-cyclohexyl-DNP were used as received from the EPA Quality Assurance Materials Bank. 2-Ethyl-DNP and 2-ethyl-nitrophenols were synthesized by stoichiometric electrophilic nitration of 2-ethylphenol (Aldrich Chemical Co., Milwaukee, WI). These materials were purified on an alumina column as needed, and product purity was assessed by gas chromatography/mass spectrometry (GC/MS). Deuteration of 2-ethyl-4,6-DNP at the phenolic function was accomplished by shaking 2-ethyl-DNP in a large excess of D_2O.

High-resolution mass spectrometry and MS/MS studies were conducted with a VG 70-250SEQ hybrid MS/MS system of EBqQ geometry; that is, a forward-geometry double-focusing sector mass spectrometer (MSI) is followed by an rf-only quadrupole collision cell with a quadrupole mass filter (MSII). A standard EI source was operated at 8 kV acceleration energy, with 70 eV nominal electron energy at a temperature of 200 °C. Direct-probe sample introduction was used for all experiments except those involving purity assessments. For GC/MS, a Hewlett-Packard (Palo Alto, CA) 5890 Series II gas chromatograph was used with a 30-m DB-5 0.32-mm i.d. capillary column split 50:1 and temperature programmed from 35 °C to 250 °C at 5 °C min with helium flow about 0.8 mL/min. Accurate mass determinations were performed at > 25,000 resolution (10% valley) by computer acquisition in the multichannel analyzer (MCA) mode, measuring the unknown peak against two mass reference peaks in perfluorokerosine.

Tandem mass spectrometry collision-activated dissociation (CAD) experiments were conducted at unit mass resolution using argon at collision energy of 20–21 eV (laboratory frame). No collision gas was present for the unimolecular experiments. All data were collected in continuum and MCA modes and smoothed after acquisition. For product ("daughter") scans, MSI was used to select the parent ion (1000 resolution) and MSII was scanned.

The photoelectron–photoion coincidence technique has been described in the literature [13, 14] but will be briefly described here. 2-Ethyl-DNP was introduced by placing solid crystals directly in the photoionization source of the instrument. Vacuum UV photons from a many-line hydrogen discharge lamp, dispersed in a 0.5-m monochromator, ionized the gaseous sample in an electric field of 10 V/cm. Photoelectrons were accelerated into a steradiancy energy analyzer [13, 14], which passes only those electrons with nominally zero initial kinetic energy. The ionic species were accelerated into a field-free region, giving a total ion flight distance of 40 cm. When an electron is detected, a start pulse is sent to a time-to-amplitude converter (TAC), and the stop pulse is signaled by the detection of an ion. The pulse-height distribution was collected and analyzed by an MCA. The ion-signal intensities were extremely small owing to the low vapor pressure of the sample.

Because the ions are detected in coincidence with zero kinetic energy electrons, the ion internal energy is given by

$$E_{int} = h\nu - IP - E_{el}$$

In this equation, $h\nu$ is the photon energy, IP is the ionization potential of the parent molecule, and E_{el} is the energy of the electron (zero in this case). Therefore, if we know the IP of the molecule, the ion internal energy is specified. This method of parent-ion energy selection provides ion appearance potentials from which dynamical fragmentation information can be derived.

Results and Discussion

The Mass Spectra

Among the many fragment peaks in the mass spectra of 2-alkyl-DNPs is one showing the unusual loss of 35 u from the molecular ion. The measured intensities of the parent, $[M - 18]^+$, and $[M - 35]^+$ ions are shown for 14 compounds in Table 1. These data illustrate several important features of the $[M - 35]^+$ formation reaction. First, $[M - 35]^+$ ions are observed only in compounds that also exhibit an $[M - 18]^+$ ion (the converse is not true). Second, $[M - 18]^+$ ions are observed only in compounds containing alkyl groups, and the alkyl group must contain more than one carbon atom for the $[M - 35]^+$ ion to be observed. Finally, the nitro group ortho to the OH participates in the reaction (note compounds **13** and **14**). The neutral losses were confirmed by high-resolution measurements to be H_2O and H_3O_2.

The role of the para nitro group was also examined. Figure 1 shows the mass chromatograms for 2-ethyl-6-nitrophenol (**13**) and 2-ethyl-4-nitrophenol (**14**). It is known [15] that on a DB-5 column *o*-nitrophenol elutes before *p*-nitrophenol and that the addition of an ethyl substituent ortho to the OH will not affect this elution order [16]. Therefore, we conclude that the species at scan 449 is the 6-nitro isomer and does in fact exhibit an $[M - 35]^+$ ion. Finally, for the species eluting at scan 648 (**14**), an $[M - 35]^+$ fragment is not observed.

Although the $[M - 35]^+$ intensity for **13** is comparable to that of compound **1**, a considerable difference in $[M]^+$ and $[M - 18]^+$ intensity is noted. These intensity differences suggest that the addition of a second nitro function on the aromatic ring significantly changes the energetics of this cation. That is, the molecule is stabilized with respect to dissociation by addition of the para nitro group. This stabilization contradicts the generally accepted view that addition of a nitro function destabilizes a cationic ring and may arise from stabilization of the radical electron.

Table 1. Mass (intensity[a]) data for $[M]^+$, $[M - 18]^+$, and $[M - 35]^+$ ions in 2-alkyl-4,6-dinitrophenols and related compounds

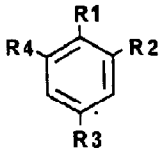

Compound	R_1	R_2	R_3	R_4	$[M]^+$	$[M - 18]^+$	$[M - 35]^+$
1	OH	Et	NO_2	NO_2	212 (100)	222 (25)	177 (40)
2	OH	*sec*-Bu	NO_2	NO_2	240 (10)	222 (2)	205 (5)
3	OH	cy-Hx	NO_2	NO_2	266 (80)	248 (35)	231 (100)
4[c]	OH	H	NO_2	NO_2	184 (100)	—[b]	—
5[c]	OH	Me	NO_2	NO_2	198 (58)	—	—
6[c]	OH	*i*-Pr	NO_2	NO_2	226 (40)	208 (1)	191 (25)
7[c]	OH	*tert*-Bu	NO_2	NO_2	240 (20)	222 (1)	205 (1)
8[c]	NO_2	H	H	H	123 (12)	—	—
9[c]	OH	Et	H	H	122 (35)	104 (1)	—
10[c]	Me	NO_2	H	NO_2	182 (1)	164 (4)	—
11[c]	OH	NO_2	H	H	139 (100)	—	—
12[c]	OH	H	NO_2	H	139 (100)	—	—
13	OH	Et	H	NO_2	167 (95)	149 (12)	132 (35)
14	OH	Et	NO_2	H	167 (98)	149 (3)	—

[a]Relative to largest peak in spectrum.
[b]Intensity below detection threshold, about 0.01%.
[c]Spectrum from National Institutes of Health reference library.

Reaction Sequence

Perhaps the most important question in any mechanistic study concerns the timing of the reaction steps and the nature of the neutral and ion structures. That is, does the neutral species consist of two products, H_2O and OH (sequential reaction), or a single product H_3O_2 (concerted reaction)? If it does proceed stepwise, what are the relative reaction rates of the individual steps? The most readily answered question concerns the nature of the neutral product. To our knowledge, the H_3O_2 molecule is not stable, except perhaps as a loosely bound adduct, nor has it ever been suggested as a neutral product in an ionic dissociation. We thus suggest the $[M - 35]$ reaction proceeds either sequentially or directly via the loss of H_2O and OH.

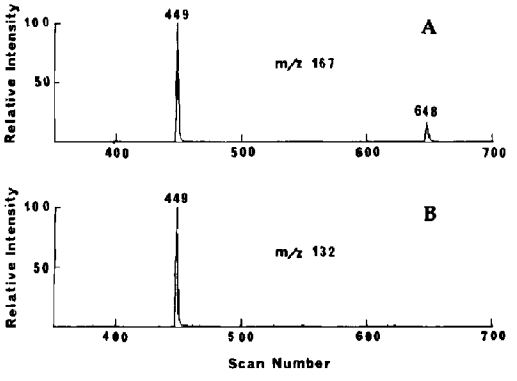

Figure 1. Ion mass chromatograms for a mixture of 2-ethyl-4-nitrophenol and 2-ethyl-6-nitrophenol. (a) m/z 167 ($[M]^+$); (b) m/z 132 ($[M - 35]^+$).

Tandem mass spectrometry was used to verify this sequential mechanism. In the first experiment, MSI was used to select molecular ($[M]^+$) ions, and MSII was scanned with no collision gas in the cell. These results are shown in Table 2. To verify that these ions were formed unimolecularly, we performed CAD experiments at several collision gas pressures. The no-gas and highest pressure (1×10^{-4} mbar) results for compound **1** are compared in Figure 2. The ratio $[M - 35]/([M - 35] + [M - 18])$ for compound **1** was extrapolated to zero pressure and gave a zero pressure ratio of 0.241. This confirms that $[M - 35]^+$ can be formed in a collision-free process.

Selecting $[M - 18]^+$ ions with MS1 produced the data shown in Table 3. The $[M - 35]^+$ intensities for the three compounds listed in Tables 2 and 3 show a revealing pattern. In both tables, the relative intensities for the $[M - 35]^+$ peaks of the three compounds are similar. This suggests that the reactions producing the $[M - 35]^+$ ions are similar. Because the $[M - 18]^+$ to $[M - 35]^+$ reactions in Table 3 refer to the loss of OH from $[M - 18]^+$, that is, the second step of a two-step process, we can infer that the $[M]^+ \rightarrow [M - 35]^+$ reaction in Table 2 is the result of a two-step process, the first involving the loss of H_2O and the second the loss of OH. That is, we conclude that the reactions are sequential. Further, the intensities of the $[M - 35]^+$ ions relative to the $[M - 18]^+$ ions in Table 3 indicate that the $[M - 18]^+$ ions are stable over only a small energy range so that most $[M - 18]^+$ ions that are formed contain sufficient energy to dissociate.

Table 2. Masses and intensities of $[M - 17]^+$, $[M - 18]^+$, and $[M - 35]^+$ product ions from metastable $[M]^+$ ions

Compound	$[M]^+$	$[M - 17]^+$	$[M - 18]^+$	$[M - 35]^+$
1	212 (100)	—	194 (20)	177 (5)
2	240 (100)	—	222 (12)	105 (20)
3	266 (100)	—	248 (18)	231 (7)

Table 3. Masses and intensities for the $[M - 34]^+$ and $[M - 35]^+$ product ions from metastable $[M - 18]^+$ ions

Compound	$[M - 18]^+$	$[M - 34]^+$	$[M - 35]^+$
1	194 (100)	178 (—)	177 (40)
2	222 (96)	206 (—)	205 (100)
3	248 (100)	232 (—)	231 (68)

These MS/MS data thus support a stepwise $[M]^+ \rightarrow [M - 18]^+ \rightarrow [M - 35]^+$ reaction in which both steps are slow, metastable processes.

The mass spectra of these compounds also show $[M - 17]^+$ fragment peaks that are too high to attribute to loss of $^{13}CH_4$. However, the $[M - 17]^+$ ions are not produced in the metastable dissociation of $[M]^+$ (Table 2). Rather, they originate from rapidly dissociating parent ions. However, some of these source-produced $[M - 17]^+$ ions are metastable and dissociate to $[M - 35]^+$ ions (Table 4). Thus a minor pathway for $[M - 35]^+$ productions appears to be via OH loss followed by H_2O loss.

In order to further examine the major reaction sequence leading to the $[M - 35]^+$ product, compound 1, deuterated at the phenolic function, was tested, and the CAD $[M]^+$ spectrum is shown in Figure 3. The parent ion (m/z 213) loses HDO (m/z 194), which then loses an OH (m/z 177). No appreciable $[M - 18]^+$ (H_2O or OD loss) is observed. Therefore, the $[M - 36]^+$ ion at m/z 177 is formed by loss of the deuterium atom in the first step, again corroborating that the reaction sequence is loss of water followed by loss of hydroxy radical.

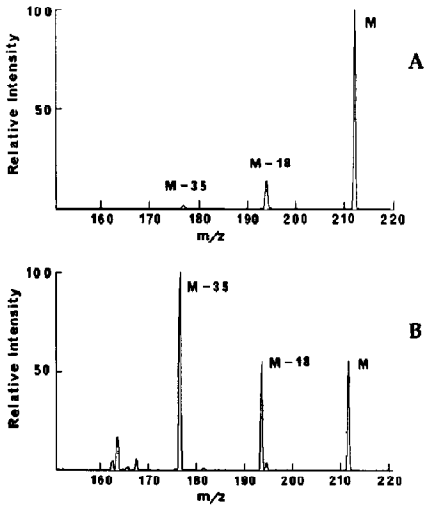

Figure 2. Comparison of MS/MS spectra of 2-ethyl-DNP at background argon pressures of (a) 10^{-8} mbar and (b) 10^{-4} mbar.

Energetics

Coincidence signals for $[M - 18]^+$ and $[M - 35]^+$ ions from compound 1 obtained by PEPICO are shown in Figure 4. As previously stated, the count rate was very low, so the signal-to-noise ratio is very small. Nevertheless, some meaningful information can be derived from the photoionization data. First, compound 1 has an ionization energy of 9.98 ± 0.08 eV, a previously unreported value. In addition, the $[M - 18]^+$ fragment ion has a lower appearance energy than the $[M - 35]^+$ ions. This is an essential experimental result that supports a sequential reaction mechanism. The observed onset for H_2O loss lies at 11.77 ± 0.08 eV. This value is, however, only an upper limit because of the kinetic shift, which is discussed below.

An observed fragment-ion onset in an experiment in which the ionizing energy is varied is not deter-

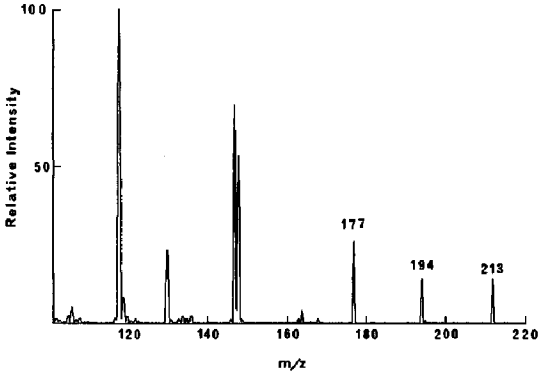

Figure 3. CAD MS/MS spectrum of 2-ethyl-D1-DNP parent ions.

Table 4. Masses and intensities for $[M - 18]^+$, $[M - 34]^+$, and $[M - 35]^+$ product ions from metastable $[M - 17]^+$ ions

Compound	$[M - 17]^+$	$[M - 18]^+$	$[M - 34]^+$	$[M - 35]^+$
1	195 (100)	194 (—)	178 (10)	177 (2)
2	223 (100)	222 (—)	206 (8)	205 (2)
3	249 (100)	248 (—)	232 (10)	231 (2)

Table 5. Vibrational frequencies (cm^{-1}) (degeneracies in parentheses) used for the RRKM rate calculation

2-Ethyl-DNP$^+$					
	3082 (8)	1439 (14)	1149 (7)	855 (13)	584 (5)
	500 (2)	403 (4)	261 (4)	171 (4)	70 (2)
$[M]^+ \rightarrow [M - 18]^+$ transition state					
	3082 (7)	1439 (14)	1149 (7)	855 (13)	584 (5)
	500 (2)	403 (4)	261 (4)	171 (4)	70 (2)

mined by the true dissociation limit. Instead, the observed onset represents the energy at which the reaction is sufficiently rapid for fragments to be produced prior to ion mass analysis. The difference between the observed and true fragmentation onset is called the kinetic shift [17]. For example, the kinetic shifts for phenol and nitrobenzene dissociations have been reported to be 0.4 eV and 1.56 eV, respectively [17, 18]. Using the steepest-descent algorithm [19] to determine energy state densities, a statistical theory (RRKM) rate was calculated for $[M - 18]^+$ formation from compound 1. The vibrational frequencies estimated from those of nitrobenzene [20], methanol [21], and ethyl bromide [22] are shown in Table 5. The transition-state frequencies were taken to be the same as the molecular ion frequencies, with one C—H stretch removed for the H-atom rearrangement coordinate. This allowed the assumed activation energy to be varied until the rate at the observed fragmentation onset (1.79 eV parent ion internal energy) was 10^4 s^{-1}, a rate previously found to correspond to the PEPICO onset [17]. This calculation yields the dissociation energy for the water loss of 1.10 eV. The difference between the observed onset at 1.79 eV and the dissociation energy gives a kinetic shift of 0.69 eV for this reaction.

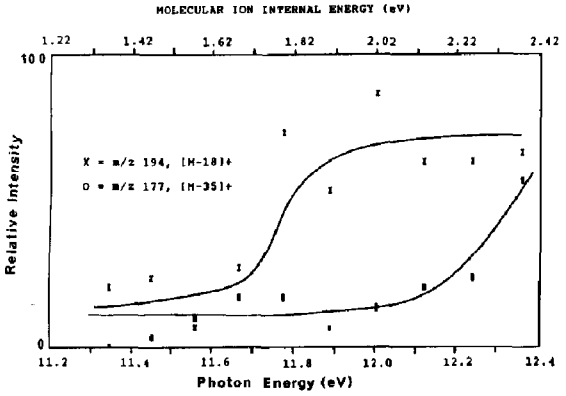

Figure 4. PEPICO signals as a function of photon energy and $[M]^+$ internal energy for compound 1.

The barrier height for the second reaction step ($[M - 18] \rightarrow [M - 35]$) is more difficult to obtain, but useful information can be derived. The onset for $[M - 35]^+$ ion formation occurs when the molecular ions are prepared with approximately 1.9 eV, which indicates that the upper limit for $[M - 18]^+$ internal energy is about 0.80 eV. This value is an upper limit because kinetic energy released during $[M - 18]^+$ formation was not determined in this experiment. The presence of a second barrier suggests that the $[M - 18]^+$ ions reside in a potential minimum. However, the second barrier is considerably smaller than the first.

Since the mass spectra described in Table 1 were obtained at 70-eV electron energy, the average molecular ion internal energy content can easily exceed 2 eV. At higher molecular ion internal energies, the $[M - 18] \rightarrow [M - 35]$ reaction is expected to dominate, with the $[M - 18]^+$ ion representing a relatively short-lived intermediate in the $[M] \rightarrow [M - 35]^+$ reaction. This is shown diagramatically in Figure 5. If an ion is made with approximately 12 eV total energy, dissociation to $[M - 18]^+$ occurs readily, because the energy is nearly 1 eV above the dissociation energy. On the other hand, the subsequent loss of OH is considerably less likely, because the total energy is now only 0.2 eV above that dissociation limit. In addition, some of the excess energy available to the $[M - 18]^+$ ion will be lost through translation and internal energy of the H_2O. However, at higher total ion energies, the energy deposited in the $[M - 18]^+$ ion will exceed the dissociation limit so that the $[M - 35]^+$ ion becomes dominant. This is consistent with the general trend in Table 1, that at 70 eV the $[M - 35]^+$ intensities are greater than the $[M - 18]^+$ intensities.

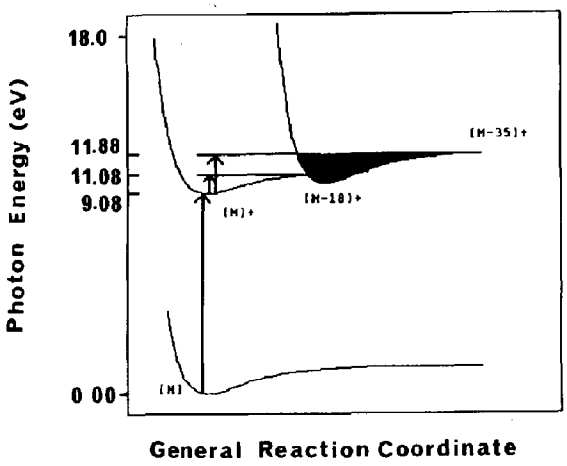

Figure 5. Diagramatic representation of the energetics of the $[M - 35]^+$ formation reaction. The shaded area indicates the region where $[M - 18]^+$ ions are stable.

Reaction Mechanism

The proposed sequence of steps leading to both $[M - 18]^+$ and $[M - 35]^+$ products is shown in Scheme I. The mechanism consists of two sequential reactions mediated by the ortho effect. In the first step, a hydrogen atom from the alkyl group is transferred to the OH via a six-membered ring. In the process, an intermediate ion–dipole complex (structure **15** in Scheme I) is formed between the bicyclic ion and the neutral dipolar water molecule. Such an intermediate would then lose the water molecule with little reverse activation energy. The formation of an ion–dipole complex between water and the bicyclic ion is perhaps similar to the production of cyclopropane ion during water loss from the propanol ion [23]. In that reaction, the cyclopropane ion rather than the lower energy propene ion is formed. The first step in the $[M]^+$ to $[M - 18]^+$ reaction, the actual H rearrangement, may gain an additional driving force from anchimeric assistance [24]. The bicyclic $[M - 18]^+$ ion (structure **16**) would not be very stable if the R group were a CH_3, a fact that is consistent with the absence of $[M - 18]^+$ (and $[M - 35]^+$) ions in the fragmentation of 2-methyl-DNP ions (compound **5**). This is also consistent with the absence of similar ortho effects in methylnitrobenzene [25].

In the proposed mechanism of Scheme I, the first step in the loss of OH from the $[M - 18]^+$ ion involves donation of an H atom by the alkyl group to one of the O atoms in the nitro group. Another six-membered ring intermediate (structure **17**) leads to the transient ion **18**, from which OH loss follows by a simple bond cleavage. The participation of the alkyl group is clearly important in this reaction. Only parent ions that first lose H_2O react further via OH loss. It seems reasonable that the H atom for the OH loss also comes from the alkyl group. Structure **18** is clearly not a long-lived species. This we deduce from the fact that the CAD spectra of the $[M - 18]^+$ ions do not show any loss of the NO_2H group. The NO_2 loss channel is, however, clearly evident (see Table 6).

Other mechanisms have been proposed for OH loss from alkylnitroaromatic compounds. For example, Depke et al. [26] studied the loss of OH from *o*-nitrostyrene ions, a reaction that is similar, but not identical, to the $[M - 18] \rightarrow [M - 35]$ reaction under discussion here. Deuterium labeling experiments by these workers showed the majority of OH loss intensity resulted from transfer of a β hydrogen, but the transfer of an α hydrogen was also significant. Further, these workers proposed a rather involved five-step mechanism for this reaction that includes a nitro-to-nitrite rearrangement, a NO transfer to the β-ethenyl carbon through a seven-membered cyclic transition state, an H-atom transfer via Beckmann rearrangement, finally followed by OH loss yielding ion **20**.

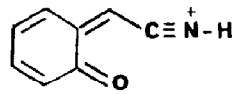

20

Such a mechanism might apply to the OH loss from the $[M - 18]^+$ formed from 2-alkyl-4,6-DNP ions. However, because this ion has one less aromatic hydrogen atom than the *o*-nitrostyrene ion, there seems little justification for proposing such a mechanism in this case. In addition, the $[M - 17]$ ions produced from *o*-nitrostyrene ions lost HCN in a CAD experiment, whereas the $[M - 35]^+$ did not undergo such a reaction in the present CAD experiments. Therefore, in the absence of detailed labeling experiments, we adopt the simpler, more direct mechanism of OH loss discussed above.

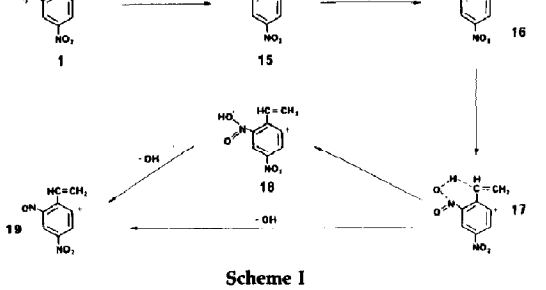

Scheme I

Table 6. Masses and intensities for $[M - 64]^+$ and $[M - 65]^+$ ions produced from CAD of $[M - 18]^+$ ions

Compound	$[M - 18]^+$	$[M - 64]^+$	$[M - 65]^+$
1	194 (100)	148 (18)	147 (—)
2	222 (75)	176 (13)	175 (—)
3	248 (100)	202 (10)	201 (—)

The only stable structure in Scheme I that can be detected is the intermediate $[M - 18]^+$. Several possible structures for this ion were considered. First, it is possible that the alkyl chain becomes incorporated in the ring, yielding a substituted cyclooctatetrane (COT) structure. Smith et al. [27] report that the barrier for this isomerization is between 0.9 and 1.2 eV above the COT ionic ground state. This places the isomerization barrier between 12.0 and 12.3 eV, using 11.1 as the COT ionic ground-state energy [28]. The lower value, 12.0 eV, is close to the observed appearance energy for $[M - 35]^+$; however, when the nonselective nature of the $[M - 18]^+$ ion is considered (recall that 11.9 eV was an upper limit for the $[M - 35]^+$ true onset) and because nitro groups on the aromatic ring in general raise reaction barriers [29], it is reasonable to conclude that this rearrangement does not occur at the energies studied. However, isomerization to a COT structure after OH loss is a possible structure for the $[M - 35]^+$ ion.

There are several experiments that could be carried out to test the proposed mechanism. First, the mass spectra of 2-CD_2CH_3-DNP would demonstrate which H (D) atom is transferred to the OH group in the initial H_2O loss step. If the H atoms are not totally scrambled, it may be possible to test the second step as well. The synthesis of the labeled compounds is beyond our capabilities at the present time. In addition, further investigation is necessary to determine the nature of rearrangement for the second step, that is, is the NO rearranging as in *o*-nitrostyrene [28], is there an oxygen migration, or is there merely a hydrogen transfer? Labeling experiments may not directly yield this information, because these experiments give insight only into what atoms are lost according to their initial positions in the structure.

Conclusion

The 2-alkyl-4,6-DNPs have been found to undergo an unusual unimolecular reaction, fragmentation to $[M - 35]^+$. In this report, we propose a mechanism for this fragmentation process, two sequential reactions that are each a concerted rearrangement process. These two reactions, loss of neutral H_2O and loss of OH radical, are examples of ortho effects. In addition, we have determined that this is a low-energy fragmentation, with $[M - 35]^+$ ions being formed when total molecular ion internal energy is as low as 2 eV. Isotopic labeling of the phenolic H atom confirms that this atom is lost in the initial H_2O expulsion without hydrogen scrambling. The study of several 2-alkyl-4,6-DNPs demonstrates that alkyl (greater than CH_3) and nitro groups must be in the ortho position. On the basis of these results, we conclude that the $[M - 35]^+$ fragment ion is a useful marker for the presence of 2-alkyl-4,6-DNPs, which include several environmentally significant pesticides.

Acknowledgment

We are grateful to NSI Technology Services Corporation for support of this work. We would also like to thank Professor M. Bursey of the University of North Carolina at Chapel Hill and Professor H. Schwarz at the Institut für Organische Chemi, Technische Univerität Berlin, for several helpful discussions. This work was supported in part by a grant from the Department of Energy.

References

1. McLafferty, F. *Interpretation of Mass Spectra*, 3rd ed.; University Science: Mill Valley, 1980; Chapter 9.
2. Ramana, D.; Rama Krishna, N. V. S. *Org. Mass Spectrom.* **1989**, *24*, 317.
3. Ramana, D.; Viswanadham, S. *Ind. J. Chem.* **1988**, *27B*, 613.
4. Ramana, D.; Rama Krishna, N. V. S. *Org. Mass Spectrom.* **1989**, *24*, 66.
5. Baldwin, M.; Bowley, H. *Org. Mass Spectrom.* **1982**, *17*, 580.
6. Beynon, J.; Saunders, R.; Williams, A. *The Mass Spectra of Organic Molecules*; Elsevier: New York, 1968; p 327.
7. Meyerson, S.; Puskas, I.; Fields, E. *J. Am. Chem. Soc.* **1966**, *88*, 4974.
8. Kulkarni, P.; Kamath, H.; Kulkarni, S. *Org. Mass Spectrom.* **1984**, *19*, 334.
9. Ramana, D.; Sundaram, N.; George, M. *Org. Mass Spectrom.* **1989**, *24*, 63.
10. Ramana, D.; Viswanadham, S. *Org. Mass Spectrom.* **1983**, *18*, 162.
11. Vouros, P.; Peterson, B.; Dafeldecker, W.; Neumeyer, J. *J. Org. Chem.* **1977**, *42*, 744.
12. Mallen, D.; Smith, J. *Org. Mass Spectrom.* **1979**, *14*, 171.
13. Baer, T.; Peatman, W.; Schlag, E. *Chem. Phys. Lett.* **1969**, *4*, 243.
14. Baer, T. In *Gas Phase Ion Chemistry*; Bowers, M. F., Ed.; Academic: New York, 1979; Vol. 1, Chapter 5.
15. Hynning, P.-P., Remberger, M.; Nielson, A. H. *J. Chromatog.* **1989**, *467*, 99.
16. Albro, P. W. NIEHS Research Triangle Park, NC; Personal communication.
17. Faser-Monteiro, M.; Fraser-Monteiro, L.; DeWit, J.; Baer, T. *J. Phys. Chem.* **1984**,*88*, 3622.
18. Baer, T.; Morrow, J. C.; Shao, J. D.; Olesik, S. *J. Am. Chem. Soc.* **1988**, *110*, 5633.
19. Forst, W. *Theory of Unimolecular Reactions*; Academic: New York, 1973; Appendix.
20. Green, J.; Harrison, D. *Spectrochim. Acta* **1970**, *26A*, 1925.
21. Shimanouchi, T. *Natl. Stand. Ref. Data. Ser.* (U.S. Natl. Bur. Stand.) **1972**, *NSRDS-NBS 39*, 107.
22. Shimanouchi, T. *Natl. Stand. Ref. Data. Ser.* (U.S. Natl. Bur. Stand.) **1972**, *NSRDS-NBS 39*, 168.
23. Shao, J.-D.; Baer, T.; Morrow, J. C.; Fraser-Monteiro, M. L. *J. Chem. Phys.* **1987**, *87*, 5242.
24. Morrison, R.; Boyd, R. *Organic Chemistry*, 5th ed.; Allyn and Bacon: Boston, 1987; Chapter 20.
25. Butcher, R.; Thomas, C. *Org. Mass Spectrom.* **1979**, *14*, 448.
26. Depke, G.; Klose, W.; Schwarz, H.; Blum, W.; Richter, W. J. *Org. Mass Spectrom.* **1983**, *18*, 568.
27. Smith, D.; Baer, T.; Willett, G.; Ormerod, R. *Int. J. Mass Spectrom. Ion Processes* **1979**, *30*, 155.
28. Batich, C.; Bischof, P.; Heilbronner, E. *J. Electron. Spectrosc. Relat. Phenom.* **1972/73**, *1*, 333.
29. Morrison, R.; Boyd, R. *Organic Chemistry*, 5th ed.; Allyn and Bacon: Boston, 1987; Chapter 14.